

Surface parameterization and registration for statistical multiscale atlasing of organ development

F. Selka¹, J. Burguet¹, E. Biot¹, T. Blein², P. Laufs¹ and P. Andrey¹

¹ Institut Jean-Pierre Bourgin INRA, AgroParisTech, CNRS,
 Université Paris-Saclay, F-78000 Versailles, France

² Institut des Plantes Paris-Saclay, Gif-sur-Yvette, France

selka.faical@gmail.com

Abstract

During organ development, morphological and topological changes jointly occur at the cellular and tissue levels. Hence, the systematic and integrative quantification of cellular parameters during growth is essential to better understand organogenesis. We developed an atlasing strategy to quantitatively map cellular parameters during organ growth. Our approach is based on the computation of prototypical shapes, which are average shapes of individual organs at successive developmental stages, whereupon statistical descriptors of cellular parameters measured from individual organs are projected. We describe here the algorithmic pipeline we developed for 3D organ shape registration, based on the establishment of an organ-centered coordinate system and on the automatic parameterization of organ surface. Using our framework, dynamic developmental trajectories can be readily reconstructed using point-to-point interpolation between parameterized organ surfaces at different time points. We illustrate and validate our pipeline using 3D confocal images of developing plant leaves.

1. Introduction

In living organisms, organ morphogenesis results from the spatio-temporal integration of processes at various scales (genetic, cellular, tissular). During growth, these mechanisms induce cell morphological and topological changes that contribute to the evolution of the organ shape. In turn, shape transformations can impact at the cellular level. Hence, quantifying the joint dynamics at the cellular and organ levels is essential to better understand organogenesis [1] [12] [7]. One challenge is in particular to detect the emergence of cell populations with distinct characteristics that accompany the transformation of organ shape. A framework was recently proposed to systematically quantify cells over the organ surface by generating individual

maps of 3D cell morphological and topological parameters using fixed samples at different developmental stages [10]. The use of fixed specimens provides the high cell resolution requested for quantitative analysis at the organ scale. However, inter-individual variability [11] can hide meaningful patterns in these individual maps. Furthermore, the use of fixed samples is a bottleneck to visualize and identify the dynamics of the cellular growth [1]. To address these issues, we propose to integrate individual maps into statistical atlases showing the spatial distribution of cellular parameters over average organ shapes. Our strategy is based on surface registration and averaging to compute prototypical shapes. Here, we describe the automated surface parameterization method that makes the core of this approach. We chose the developing leaf of the model plant *Arabidopsis thaliana*, which follows stereotyped growth trajectories at the organ scale, as a challenging system for studying organ morphogenesis. Indeed, leaves develop in three dimensions and undergo complex shape changes during their growth [4](Fig. 1A).

2. Material and Methods

2.1. Experimental data

Developing leaves were dissected, fixed, stained and imaged using a confocal microscope, thus providing images of cellular walls at the whole organ scale (Fig. 1). Images were segmented using a 3D watershed algorithm (Fig. 2B, Left). Non-epidermal cells were merged into a unique “sub-epidermal” label. In this work, we focus our analysis on epidermal cells only since the epidermis plays a key role in leaf morphogenesis [6].

2.2. Overview of the method

Because individual leaves can be twisted (Fig. 1A), defining an organ centered coordinate frame cannot rely on straight axes and canonical planes [2]. We propose instead

an approach that closely follows the actual organ shape in the determination of organ axes. Leaves are characterized by two distinct upper (adaxial) and lower (abaxial) sides and exhibit bilateral symmetry [4]. We thus define a leaf centered coordinate system based on two axes: the first one is the boundary between the two sides, the second one corresponds to the left/right limit. In transversal views, developing leaves can be roughly assimilated to triangular shapes, with the adaxial side representing the base of the triangle and the two halves of the abaxial side corresponding to the two other sides of the triangle (Fig. 1B). Our surface parameterization method thus proceeds in three steps: (1) partitioning of the leaf surface into three domains corresponding to the adaxial side and the two halves of the abaxial side; (2) generation of a leaf centered coordinate system, providing four quarters; (3) parameterization of each quarter. Using this parameterization, average shapes with average cell measurements can be computed and interpolated between successive stages. The algorithms presented in this paper were implemented in C++ and were integrated into our in-house libraries.

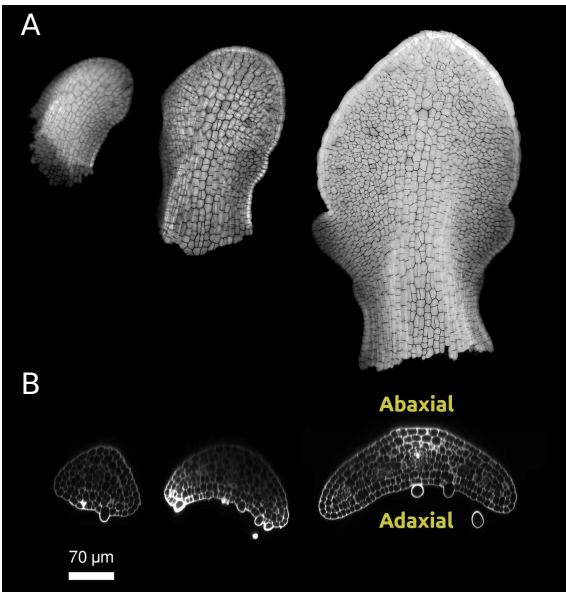


Figure 1. 3D confocal images of fixed leaves at three different developmental stages. (A) 2D average intensity projections. (B) Transverse sections.

2.3. Partitioning of the leaf surface

A preliminary approach to split the cell population into two groups corresponding to the adaxial and abaxial sides was described in [10]. In that method, for each epidermal cell i , a normal vector \vec{N}_i pointing along the cell thickness (orthogonal to the interface with sub-epidermal cells) was computed (Fig. 2B, Middle). A partitioning of the leaf surface was obtained through a clustering of the set $\{\vec{N}_i\}$ of

direction vectors. The standard K-means clustering algorithm was used to split the cell population into two adaxial and abaxial groups. However, the non-deterministic nature of the K-means algorithm affects the reproducibility of the clustering [9] (Fig. 2A), because of the random selection of data points as initial cluster centroids. Besides, our classification must be carried out in an unambiguous way, since as described in Sec. 2.2 we need to identify and distinguish between the class representing the adaxial cells (base of the triangle) and the other two classes representing the two halves of the abaxial cells (the two other sides of the triangle).

For these purposes, we propose here to pre-compute the initial centroids from a first round of clustering which will allow an identification of the classes and ensure a robust classification. The K-means algorithm is first applied with $K = 2$ to split $\{\vec{N}_i\}$ into two sets $\{\vec{N}_i^1\}$ and $\{\vec{N}_i^2\}$ corresponding to the abaxial and adaxial cell populations. The K-means algorithm is then run independently on each subset with $K = 2$. The centroid of each of the four resulting ensembles is computed. Let C'_1, C''_1 be the pair of centroids corresponding to the first set $\{\vec{N}_i^1\}$ and C'_2, C''_2 the pair of centroids for the second set $\{\vec{N}_i^2\}$. Because of the globally triangular appearance of the leaf in transverse sections, the pair of centroids C'_{i^*}, C''_{i^*} with the maximum Euclidean distance are interpreted as corresponding to the two halves of the abaxial side. The average of the two other centroids C'_{j^*}, C''_{j^*} ($j^* = 1 + i^* \bmod 2$), corresponding to the adaxial side, is computed. The obtained three centroids are used as initial cluster centroids in a final run of the K-means algorithm ($K = 3$) on the initial set of direction vectors $\{\vec{N}_i\}$. Fig. 2B shows the resulting partitioning of leaf surface into three classes. Running the whole procedure several times on each leaf produced an invariant partitioning.

Merging the two sets of the abaxial side provides a separation of the epidermal cell population in two adaxial and abaxial populations, the frontiers of which correspond to the leaf margin. We quantitatively compared the performance of the proposed approach against the one described in [10], using manual annotations of leaf sides on six different leaves by four biological experts. Compared with expert annotation, the error rate was 3.85% for the approach described in [10] while it dropped at 2.62% with the approach proposed here. Hence, improving the robustness of the partitioning procedure also provided a more accurate side separation.

2.4. Computing an organ centered coordinate system

We establish a leaf-centered coordinate system by computing two perpendicular axes: a lateral axis, corresponding to the separation between the adaxial and abaxial sides, and

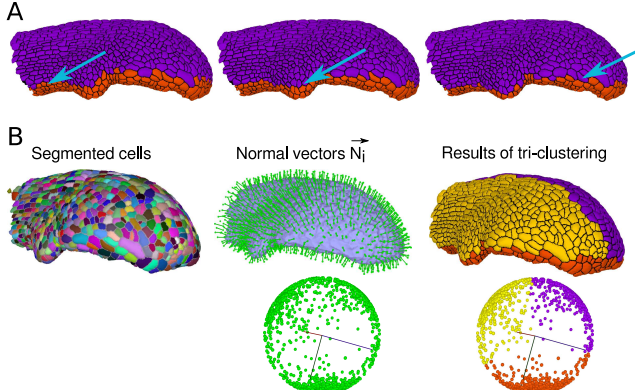


Figure 2. Surface partitioning based on clustering of normal vectors. (A) Partitioning into two classes using the classical K-means. Blue arrows point to cells that are assigned to a different side between different runs of the method described in [10]. (B) Partitioning into three classes (adaxial side and left/right abaxial side).

a longitudinal axis, corresponding to the bilateral axis of symmetry of the leaf (Fig. 3A).

Computation of the lateral axis. The lateral axis is represented as a curve with ordered points that define the margin between the adaxial and abaxial sides (Fig. 3A). We firstly compute all the points that are at the margin between the abaxial and the adaxial sides and retain only those that are at the leaf surface. Based on mathematical morphological operators, we automatically determine the petiole section of the leaf (Fig. 3C), which corresponds to the position where the leaf was separated from the plant. Let P be the barycenter of the petiole section and A the tip (apex) of the leaf, obtained as the margin point that is the farthest from P (Fig. 3D). Based on its relative positioning to P and A , and on the identification of the adaxial and abaxial side, each margin point is assigned to the left or right leaf margin.

Let I_0^L and I_0^R be the closest margin points to P on each lateral (left or right) side, respectively (Fig. 3C). The computed points which define the margins between the adaxial and abaxial sides are not ordered. We designed a procedure reminiscent of the Douglas-Peucker algorithm [5] to compute two smooth margin curves with ordered points connecting I_0^L and I_0^R to the apex A . The algorithm is based on the following condition: if the farthest point from the line segment defined by the current first and last points is greater than ϵ then that point must be kept. Starting from A and I_0^L (or I_0^R), the procedure is applied recursively until no additional point satisfy the condition. This allows a robust extraction of the margin contour as a connected curve. Finally, the points of the two curves are resampled uniformly with the same number of points on each side (see in Fig. 3C the curves defined by red dots).

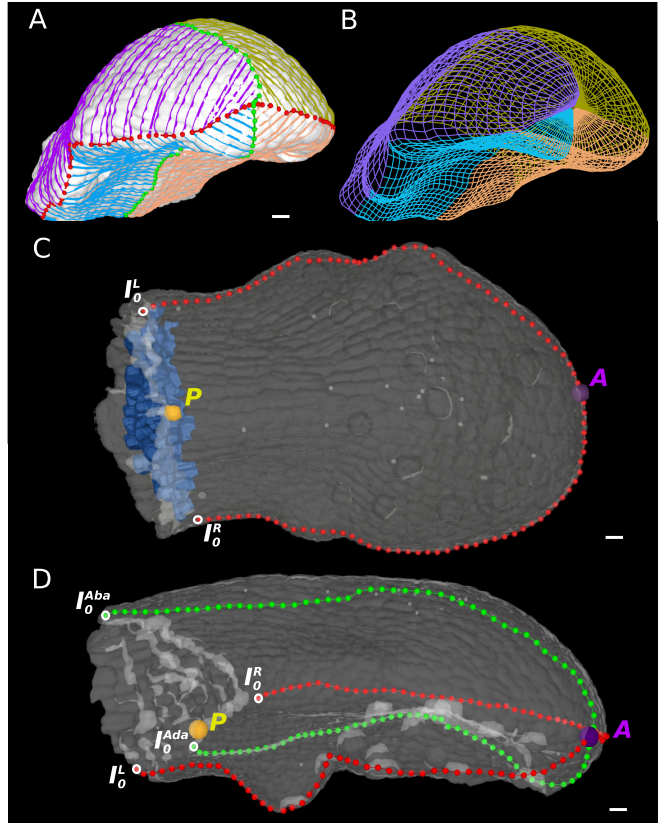


Figure 3. Overview of the surface parameterization method. (A) Coordinate system defined by two axes: a lateral axis (Red), corresponding to the interface between adaxial and abaxial sides; a longitudinal axis (Green), corresponding to the bilateral symmetry axis of the leaf. Colored segments: geodesic paths between points at homologous curvilinear coordinates on the axis curves. (B) Parameterization of leaf surface using a quadrangular mesh. (C) Leaf surface (Transparent grey) with petiole section in blue and computed anatomical landmarks. P petiole; A tip (apex); I_0^L , I_0^R closest points to P on the left and right margins, respectively. (D) Leaf surface (Transparent grey) with computed anatomical landmarks. I_0^{Aba} , the closest point to P on the boundary of the two halves of the abaxial side. I_0^{Ada} the projection of the middle of segment $[I_0^L I_0^R]$ onto the adaxial side. Scale bars: $10\mu m$.

Computation of the longitudinal axis. The longitudinal axis is defined by two curves splitting each side in two halves. The first one is obtained by applying the procedure described above for the lateral axis to the interface points between the two lateral halves of the abaxial side. This curve starts at I_0^{Aba} , the closest point to P , and ends at A (see in Fig. 3D the curves defined by green dots).

The second curve is obtained by projecting the medial axis of the two lateral curves onto the adaxial side. Indeed, the clustering of the normals at the adaxial side does not allow to obtain a separation in two halves due to the lower curvature of the adaxial side compared to the abaxial one.

Thus, the second curve in the adaxial side is computed by projecting the center of for each segment $[I_i^L I_i^R]$ onto the adaxial side. Connecting the resulting ordered set of projected points provides the desired polygonal curve.

Finally, the two resulting polygonal curves of the longitudinal axis are resampled into the same number points used for the lateral axis.

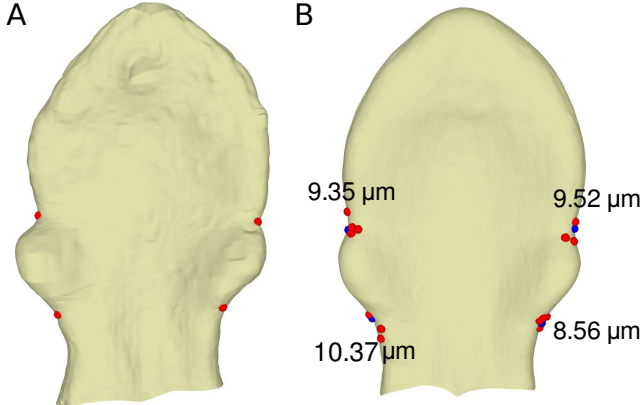


Figure 4. Organ surface registration and averaging: quantitative evaluation. (A) Individual leaf with manual landmarks (Red). (B) Average leaf ($n = 11$) with manual landmarks (Blue) and automatically registered landmarks from individual leaves (Red). Numbers are average registration errors.

In the end, this approach provides four polygonal curves that define our organ centered coordinate system.

2.5. Averaging shapes and cell measurements

The centered coordinate system defines four quarters, which correspond respectively to the left and right halves of the adaxial and abaxial sides of the leaf. For each quarter, a quadrangular mesh is built by first connecting points at homologous curvilinear coordinates on the two sides (one lateral, one longitudinal) of the quarter. This is done along geodesic paths to ensure the preservation of leaf shape (Fig. 3A). These paths are then uniformly resampled into a fixed number of points, thus providing the quarter quadrangular parametric surface (Fig. 3B).

Since the computed parameterized surfaces have the same number of points and are defined in a standardized coordinate system, we use the methods described in [8] in order to register and compute an average leaf shape. This algorithm performs a groupwise registration between several individuals represented each by several surfaces. Let $S_i^k = \{x_i^k(u, v), y_i^k(u, v), z_i^k(u, v)\}$ be the quadrangular surface of the k^{th} ($k \in \{1, \dots, 4\}$) quarter in the i^{th} leaf. The registration of N leaf surfaces is obtained by iteratively combining averaging and pairwise registration to the average shape in order to determine for each leaf i the transformation T_i that minimizes the following error function [8]: $E(T_1, \dots, T_N) = \sum_{i>j} \sum_{k=1}^4 \|T_i(S_i^k) - T_j(S_j^k)\|^2$. The

average shape was obtained by averaging the four quarters across the registered leaves.

We integrated cellular parameters into average shapes over sets of leaves from identical developmental stages. The leaf length was considered as a proxy of time development. In each individual leave several cell parameters were computed for each epidermal cell. The average map of cell parameters was obtained by computing, for each vertex of the average shape, the corresponding vertices in the individual shapes and by averaging the parameter values of the cells found at these positions.

2.6. Reconstructing dynamic growth trajectories

Since our method relies on an automatic surface parameterization computation using a common coordinate system, a dynamic developmental trajectory can be readily computed by registering and interpolating the average parameterized surfaces at different stages of development based on point-to-point correspondences. First, we automatically registered the average shapes of the different developmental stages using the ICP algorithm (rigid transformation) [3] to correct for differences in orientation. Next, differences in absolute positioning were rectified by translating the petiole barycenter P to the same position for all average surfaces. Finally, a point-to-point linear interpolation was performed to compute dynamic organ and cellular parameters trajectories.

3. Results

In this section, we firstly assess the accuracy and robustness of the proposed method. Secondly, we show the interest of using systematic and integrative quantification approaches to analyze cellular parameters during growth. Finally, we illustrate the feasibility of the method to reconstruct a dynamic developmental organ trajectory that allows by-passing the limitations of having to process fixed samples.

3.1. Validation

To evaluate the registration accuracy of the proposed method, we selected 11 individual leaves with length comprised between 300 and 400 μm , representing approximately a one-day window of growth. This window of growth encompasses significant global (organ growth) and local shape (teeth growth) deformations, thus representing particularly demanding conditions for validation. We manually annotated four remarkable landmarks on each parameterized leaf surface (Fig. 4A) and on the average leaf shape (Fig. 4B). These landmarks correspond to the sinuses of the teeth on the leaf where they undergo a large deformation during the growth of the organ (leaf serration). Following shape registration and averaging, we computed for each

landmark the average distance between positions from individual registered leaves and the position on the average shape (Fig. 4D). The results shows an average error of $9.45 \mu\text{m}$, corresponding to an error of at most two cells.

3.2. Inter-individual registration and integration

Figure 5 illustrates the mapping of the cellular parameters (volume and thickness) onto individual and average leaf shapes. Five individual leaves at the same developmental stage corresponding to lengths around $400 \pm 15 \mu\text{m}$ were used.

Inter-individual variability hampers the detection of clearly defined patterns on the individual representations. On the contrary, the integration of the individual measures into the average representation shows a well delineated pattern of cellular parameter variations over the leaf surface, suggesting a morphological patterning of epidermal cells. As illustrated by the comparison between the patterns of cell volume and cell thickness, different parameters generally corresponded to a specific pattern. Specific morphological cell signature were associated with the shaping of the leaf. For example, the average map of cell thickness revealed that cells associated to leaf teeth had a lower thickness than cells in other regions of the leaf. In addition, the average representation of cell volume revealed a group of cells at the apex of the leaf that exhibited a smaller size compared to the surrounding cells (Green circle in Fig. 5A). These cells had not been identified in the first place in the individual leaves. This emphasizes the benefit of average parametric maps and their ability to reveal shared patterns between individuals that can be hidden by inter-individual variability.

3.3. Dynamic atlasing and quantification

Figure 6 illustrates the mapping of the cell volume onto average leaf shapes at different stages of development, where multiple individual leaf shapes at each developmental stage were used to compute the average shape with the corresponding average values. Using the method described in Sec. 2.6 we computed a dynamic atlas (4D map) where we can correlate the morphological transition at the organ scale with the dynamics of the cellular parameters during growth. The complete movie can be found at the link: [Shapes-Interpolation](#), where the average shapes showed in the Fig. 6 are interpolated. The reconstructed trajectories allow us further identification for the emergence of a specific cell populations which is associated with the shaping of organs.

4. Conclusion

In this paper, we described a strategy based on surface parameterization, registration and averaging to integrate cellular parameters into statistical maps at the organ

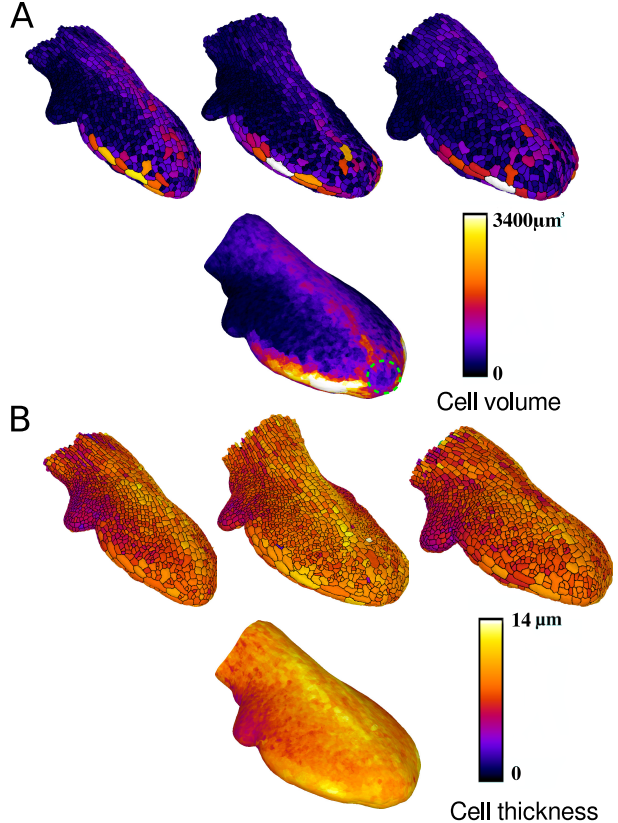


Figure 5. Surface rendering of parametric maps: (A) cell volume. (B) cell thickness *Top*: Color-coded rendering of cell parameters in sample individual leaves. *Bottom*: Average leaf shape ($n = 5$) with average cell parameter values. Green circle: small group of cells at leaf tip with low cell volume.

scale. The obtained statistical representations are representative of the populations of shapes and provide atlases of cellular parameters that will allow to correlate cell growth to the evolution of organ shape during its development. We believe these statistical atlases will be useful to extract robust principles and to elucidate the multiscale processes that subtend organ morphogenesis. Using the proposed method of surface parameterization, organs can be interpolated, thus providing dynamic atlases of cellular parameters. This allows by-passing the limitations of having to image fixed rather than live samples because of lack of accessibility or because of too large size and depth. In the case where live imaging data would be available, our approach would also be useful to reconstruct dense trajectories from sparsely sampled time-points. Local gradients computed over these dynamic trajectories and multivariate statistics will be useful to automatically delineate cell populations with distinct characteristics and thus decipher the dynamics of cellular growth during development. Lastly, the obtained results can be used for the development of a cell model to investigate how cellular parameters contribute to the evolution of organ

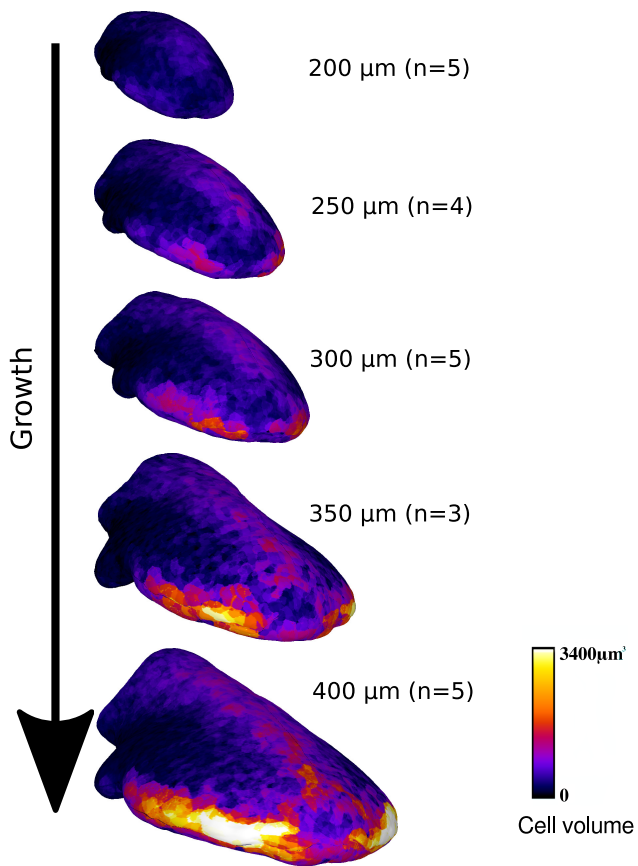


Figure 6. Surface rendering of average leaf shape at different stages of development with a color rendering of average cell volume values.

shape.

4.1. Acknowledgments

This work was supported by the "Institut de Modélisation des Systèmes Vivants" of Idex Paris-Saclay (ANR-11-IDEX-003-02) and by the Tefor Infrastructure under the Investments for the Future program of the French National Research Agency (Grant ANR-11-INBS-0014) (fundings to FS). The IJPB benefits from the support of the LabEx Saclay Plant Sciences-SPS (ANR-10-LABX-0040-SPS).

References

- [1] G. Bassel and R. Smith. Quantifying morphogenesis in plants in 4D. *Curr Opin Plant Biol*, 29:87–94, 2016. [1](#)
- [2] R. Bensch et al. Image analysis of arabidopsis trichome patterning in 4D confocal datasets. *ISBI*, pages 742–745, 2009. [1](#)
- [3] P. J. Besl and N. D. McKay. A method for registration of 3-D shapes. *IEEE Trans Pattern Anal Mach Intell*, 14(2):239–256, 1992. [4](#)
- [4] E. Biot et al. Multiscale quantification of morphodynamics: Morpholeaf, software for 2-D shape analysis. *Development*, 143:3417–3428, 2016. [1, 2](#)
- [5] D. Douglas and T. Peucker. Algorithms for the reduction of the number of points required to represent a digitized line or its caricature. *Cartographica Int. J. Geographic Inf.*, 10(2):112–122, 1973. [3](#)
- [6] S. Fox et al. Spatiotemporal coordination of cell division and growth during organ morphogenesis. *PLoS Biology*, 16(11):e2005952, 2018. [1](#)
- [7] A. Haupt and N. Minc. How cells sense their own shape—mechanisms to probe cell geometry and their implications in cellular organization and function. *J Cell Sci*, 131(6):jcs214015, 2018. [1](#)
- [8] E. Maschino et al. Joint registration and averaging of multiple 3d anatomical surface models. *Comput Vis Image Underst*, 101:16–30, 2006. [4](#)
- [9] N. Nidheesh et al. An enhanced deterministic k-means clustering algorithm for cancer subtype prediction from gene expression data. *Comput Biol Med*, 91:213–221, 2017. [2](#)
- [10] F. Selka et al. Towards a spatio-temporal atlas of 3D cellular parameters during leaf morphogenesis. *ICCVW*, 56–63, pages 56–63, 2017. [1, 2, 3](#)
- [11] L. Serra et al. Heterogeneity and its multiscale integration in plant morphogenesis. *Curr Opin Plant Biol*, 46:18–24, 2018. [1](#)
- [12] K. Sugimura et al. Measuring forces and stresses in situ in living tissues. *Development*, 143:186–196, 2016. [1](#)